STRUCTURE AND PROPERTIES OF MELT-SPUN Al-Zr-Ti ALLOYS III. PHASE TRANSFORMATIONS AT ELEVATED TEMPERATURES

PŘEMYSL MÁLEK, BOHUMIL CHALUPA, JOSEF PLEŠTIL

Rapidly solidified Al-Zr-Ti alloys are far from thermodynamic equilibrium. Electrical resistance measurements revealed two stages of microstructure changes occurring at elevated temperatures. Using the results of X-ray diffraction analysis the first stage was explained by the precipitation of the metastable $Al_3(Zr_xTi_{1-x})$ phase with $L1_2$ structure and the second stage by the formation of the stable $Al_3(Zr_xTi_{1-x})$ phase with DO_{23} or DO_{22} structure. Ti atoms substitute for Zr atoms in the lattices of these phases. This substitution improves the lattice mismatch between the particles of the $Al_3(Zr_xTi_{1-x})$ phase and the matrix and shifts the individual decomposition stages to higher temperatures. Consequently, a better structure and strength stability may be expected.

Key words: Al-based alloys for elevated temperatures, rapid solidification, phase transformations, electrical resistance, X-ray diffraction analysis

STRUKTURA A VLASTNOSTI SLITIN Al-Zr-Ti PŘIPRAVENÝCH METODOU „MELT SPINNING" III. FÁZOVÉ TRANSFORMACE U ZVÝŠENÝCH TEPLOT

Rychle ztuhlé Al-Zr-Ti slitiny jsou daleko od termodynamické rovnováhy. Měření elektrického odporu odhalila dvě stadia mikrostrukturních změn nastávajících u zvýšených teplot. Pomocí difrakce rtg. záření se podařilo vysvětlit první stadium jako důsledek precipitace metastabilní fáze $Al_3(Zr_xTi_{1-x})$ se strukturou $L1_2$ a druhé stadium jako důsledek tvorby částic stabilní fáze $Al_3(Zr_xTi_{1-x})$ se strukturou DO_{23}, resp. DO_{22}. Atomy Ti mohou substituovat atomy Zr v mříži obou fází $Al_3(Zr_xTi_{1-x})$, snižují rozdíl v mřížových parametrech mezi těmito fázemi a matricí a posunují jednotlivá stadia rozpadu k vyšším teplotám. Jako důsledek tohoto procesu lze očekávat lepší vysokoteplotní stabilitu struktury a pevnosti.

RNDr. P. Málek, CSc., B. Chalupa, Department of Metal Physics, Charles University, Ke Karlovu 5, 121 16 Prague 2, Czech Republic.

Ing. J. Pleštil, CSc., Institute of Macromolecular Chemistry, Academy of Sciences of the Czech Republic, Heyrovského nám. 1, 160 00 Prague 6, Czech Republic.

1. Introduction

Small amounts of zirconium are frequently added to commercial Al-based alloys in order to improve their mechanical properties. If the technique of chill casting is used small particles of the metastable Al_3Zr phase are formed. These particles are usually stable up to the temperatures of about 750 K, hinder lattice dislocations to move and to rearrange, suppress the static recrystallization, and stabilise the fine grain size [1]. The extremely high stability of these particles suggests the possibility to use them as the strengthening phase in the Al-based alloys designed for elevated temperature applications. In this case, however, their volume fraction has to be much higher than that used in current commercial Al-based alloys, i.e. the Zr content has to be significantly increased. The low equilibrium solid solubility of Zr in Al (about 0.05 wt.% at 700 K [2]) represents a great difficulty as coarse particles of the stable modification of the Al_3Zr phase are formed even during chill casting. Fortunately, rapid solidification techniques enable to preserve a sufficient amount of Zr in the supersaturated solid solution the following decomposition of which may result in the desired distribution of small particles of the metastable Al_3Zr phase [3, 4].

Small amounts of titanium are usually added to commercial Al-based alloys in order to refine their solidification microstructure. Coarse particles (usually of a complicated shape, chemical and phase composition) are formed and create nucleation centres for solidification. The complete suppression of the formation of these particles is very difficult in alloys with a higher Ti content, even after rapid solidification [5, 6]. Therefore, the dilute binary Al-Ti alloys do not seem to be a good basis for the development of the Al-alloys designed for elevated temperature applications.

An attempt was performed to combine both above mentioned elements for designing the Al-base alloys for elevated temperature applications. It was found that using the melt spinning method, the alloys containing 1.25 at.% (Zr + Ti) may be prepared with the phase compositions far from the thermodynamic equilibrium [7]. The small angle X-ray scattering (SAXS) experiments revealed the presence of particles with a volume fraction below 2 vol.% in the as-melt-spun alloys. The X-ray diffraction experiments showed that the particles present in the Zr-rich alloys (Zr:Ti ratio greater than 1) are preferentially formed by the metastable Al_3Zr-based phase of the structure type of $L1_2$. The Ti atoms substitute for Zr atoms in the lattice of this phase and change slightly its lattice parameter [7].

The resistance of strengthening particles to dissolution and coarsening are the prerequisites for a good structure and strength stability at elevated temperatures. The low equilibrium solid solubilities of Zr and Ti in Al and their week temperature dependence exclude a significant dissolution of strengthening particles [2]. The coarsening of strengthening particles is supposed to be diffusion controlled at

elevated temperatures. According to the model [8, 9] the coarsening rate decreases with decreasing lattice mismatch between the particles and the matrix. A partial substitution of Ti for Zr atoms reduces this mismatch and, therefore, a better high temperature stability of the size of the metastable Al_3(Zr, Ti) particles may be expected.

Numerous investigations of the decomposition behaviour of the supersaturated binary Al-Zr and Al-Ti alloys have revealed that a long term annealing at high temperatures results in the transformation of the metastable Al_3Zr and Al_3Ti phases into the stable modifications of the same stoichiometry but with another structure types (DO_{23} in the Al-Zr and DO_{22} in the Al-Ti alloys). Higher lattice mismatches of these stable modifications (see Table 1) are probably the main reason for the larger particle size of these phases and for their faster coarsening rates (e.g. [13]). Consequently, a lower strength level and a worse elevated temperature stability may be expected in alloys containing the particles of stable phases.

Table 1. Structural characteristics of the Al_3Zr and Al_3Ti phases

Phase	Stable modification		Metastable modification	
	structure	lattice mismatch [%]	structure	lattice mismatch [%]
Al_3Zr	tetragonal DO_{23}	2.9 [10]	cubic $L1_2$	0.7 [11]
Al_3Ti	tetragonal DO_{22}	5.4 [2]	cubic $L1_2$	2.0 [12]

The main objective of our investigation was to study the decomposition behaviour of the ternary Al-Zr-Ti alloys during their annealing at elevated temperatures and to clarify the influence of the partial substitution of Ti atoms for the Zr ones on the elevated temperature stability of these alloys.

2. Material and procedure

The thin Al-Zr-Ti ribbons were prepared using the melt spinning method (for details see [7]). The nominal chemical compositions corresponding at room temperature to the equilibrium phase composition of Al-5vol.% $Al_3(Zr_xTi_{1-x})$ with stoichiometric parameters $x = 1, 0.75, 0.5, 0.25$, and 0 were chosen (Table 2). The actual chemical compositions were found close to the nominal values [7].

In order to determine the temperatures of phase transformations electrical resistance measurements were carried out under the conditions of linearly increasing and decreasing temperature. At least two heat treatment cycles consisting of heating and subsequent cooling between about 300 and 800 K with constant heating and cooling rates of 10 K/min were applied for each alloy. The apparatus for this measurement is described in [14].

Table 2. Nominal chemical composition of the Al-$Al_3(Zr_xTi_{1-x})$ alloys in wt.%

x	1	0.75	0.5	0.25	0
Zr	4.1	3.1	2.1	1.0	–
Ti	–	0.55	1.1	1.65	2.2

The presence of non-matrix phases was verified by means of the small angle X-ray scattering experiments performed using a Kratky Camera equipped with a linear position sensitive detector. The measured scattering intensity was converted into the normalised intensity by means of a Lupolen standard. If the scattering curve could be extrapolated to zero scattering vector the mean square fluctuation of the scattering density $\overline{(\Delta\rho)^2}_{\mathrm{exp}}$ may be determined as [15]

$$\overline{(\Delta\rho)^2}_{\mathrm{exp}} = \frac{K}{4\pi^2}\int_0^\infty \frac{\mathrm{d}\tilde{\Sigma}}{\mathrm{d}\Omega}(q)q\mathrm{d}q, \tag{1}$$

where $\mathrm{d}\tilde{\Sigma}/\mathrm{d}\Omega$ is the normalised intensity measured with an infinitely long primary beam (smeared intensity), q is the scattering vector, and K is an instrument constant. Assuming that scattering occurs on one type of second phase particles the two-phase model predicts the relation between the scattering density $\overline{(\Delta\rho)^2}_{\mathrm{exp}}$ and the volume fraction of particles f in the form

$$\overline{(\Delta\rho)^2}_{\mathrm{exp}} = f(1-f)(\rho_{\mathrm{p}} - \rho_{\mathrm{mat}})^2, \tag{2}$$

where ρ_{p} and ρ_{mat} are scattering densities of the particle forming phase and of the matrix, respectively. The measurements were performed at samples annealed at 600, 650, and 700 K for 10 hours.

The X-ray diffraction analysis of samples annealed at 600, 650, and 700 K for up to 500 hours was performed at room temperature using Cu-K_α radiation in the diffractometer Siemens-Kristalloflex with the scanning regime 0.02°/30 s. The Si reference powder was added to some samples as an X-ray peak position standard.

3. Experimental results

Fig. 1 shows the temperature dependence of the electrical resistance for the binary Al-Zr alloy. The curve obtained during the first heating is nearly linear up to about 550 K where a large drop in resistance starts. The comparison with the second heating curve shows the irreversible character of this drop. Small differences between both cooling curves suggest that the alloy does not reach the equilibrium state even after the second heating. The third heat treatment cycle was, therefore, applied and both heating and cooling curves were found identical within the

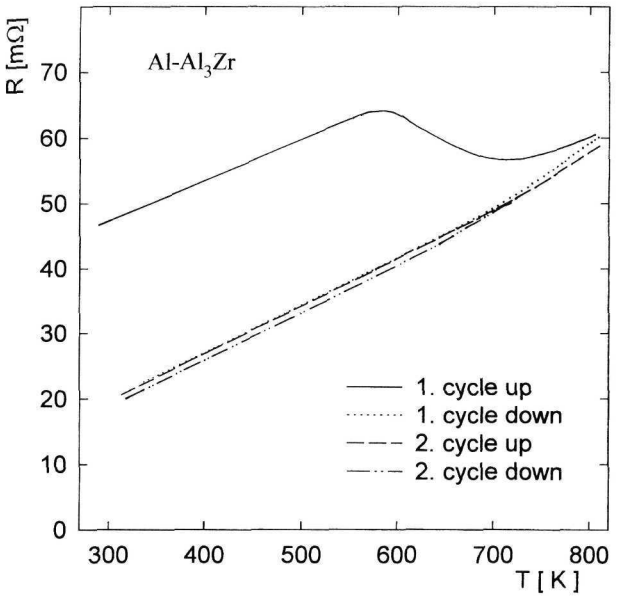

Fig. 1. Temperature dependence of electrical resistance for the binary Al-Zr alloy.

experimental scatter with the second cooling curve. The heating curves obtained both in the second and third cycles reveal a small increase in their slope at higher temperatures which seems to be reversible.

The same experiment was performed with the binary Al-Ti alloy (Fig. 2). The first heating curve seems to be linear up to about 630 K and an irreversible decrease in resistance occurs at higher temperatures. This resistance decrease is much weaker than that in the Al-Zr alloy. Similarly to the Al-Zr alloy, the processes responsible for the irreversible resistance changes are not completed even after the second heating. The influence of the substitution of Ti for Zr on the temperature dependence of resistance is shown in Fig. 3. All Zr-containing alloys exhibit a similar dependence, nevertheless, the deviation from linearity is shifted to higher temperatures with increasing Ti content.

In order to identify the position of structure changes more accurately, the true temperature coefficient of resistance α was calculated as

$$\alpha(T) = \frac{1}{R(T)} \frac{\mathrm{d}R}{\mathrm{d}T}. \tag{3}$$

The temperature dependencies of α computed from the first heating curves are plotted for selected Al-$Al_3(Zr_xTi_{1-x})$ alloys in Fig. 4. A sharp minimum in the

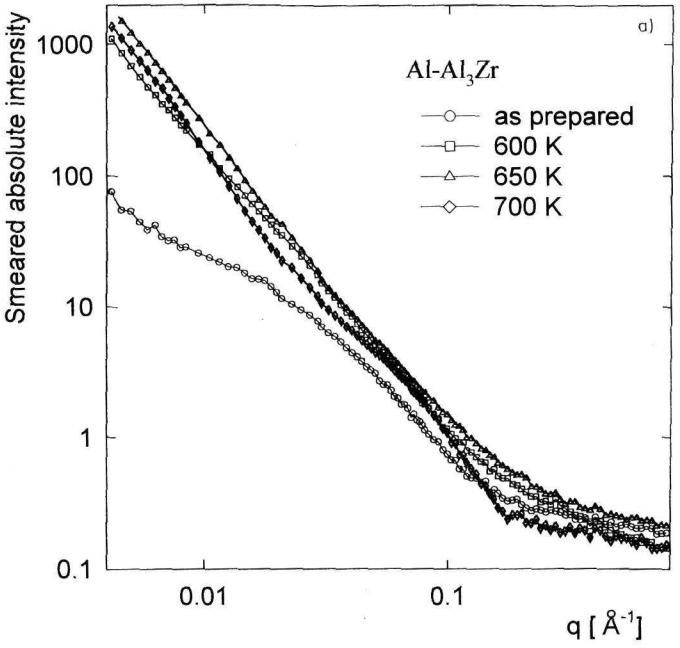
a)
Al-Al3Zr
as prepared
600 K
650 K
700 K
Smeared absolute intensity
1000
100
10
1
0.1
0.01
0.1
q [Å-1]

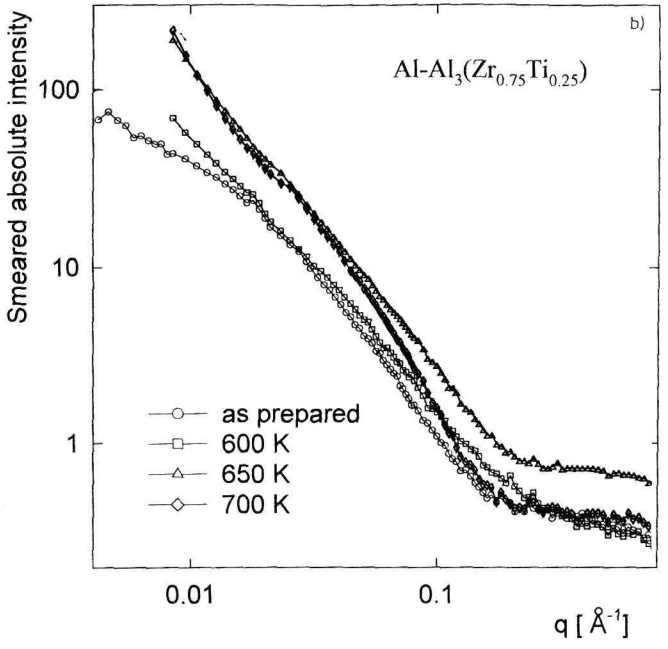
b)
Al-Al3(Zr0.75Ti0.25)
as prepared
600 K
650 K
700 K
Smeared absolute intensity
100
10
1
0.01
0.1
q [Å-1]

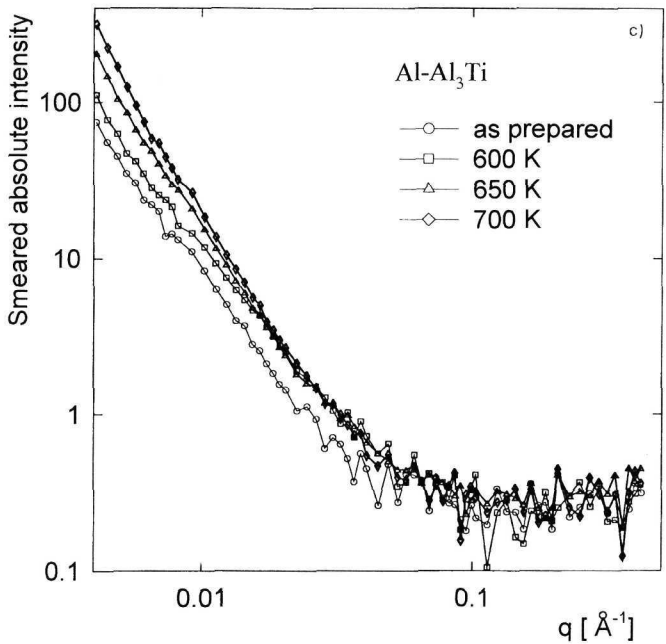

Fig. 5. SAXS curves of selected Al-$Al_3(Zr_xTi_{1-x})$ alloys annealed for 10 hours at different temperatures: a) $x = 1$, b) $x = 0.75$, c) $x = 0$.

Similarly, the changes in the term $(1 - f)$ appearing in Eq. (2) may be neglected in dilute alloys. Under these simplifications, a proportionality between the volume fraction of particles f and the scattering density $\overline{(\Delta\rho)^2}_{\text{exp}}$ may be expected. Fig. 5 shows the SAXS curves for selected alloys annealed at different temperatures for 10 hours. Excluding the as-prepared samples of the Al-Al_3Zr (Fig. 5a) and Al-$Al_3(Zr_{0.75}Ti_{0.25})$ (Fig. 5b) alloys, the scattering curves cannot be reasonably extrapolated to zero scattering vectors and the scattering density $\overline{(\Delta\rho)^2}_{\text{exp}}$ cannot be exactly evaluated. Only a very rough qualitative estimate of the changes in the volume fraction of the second phase particles due to annealing can be made. Fig. 5a shows a great difference between the scattering curves of the as-prepared sample and all annealed samples of the Al-Al_3Zr alloy. This suggests that annealing for 10 hours at the lowest temperature of 600 K already results in an increase in the volume fraction of the second phase particles. Another result was obtained in the Al-$Al_3(Zr_{0.75}Ti_{0.25})$ alloy where the SAXS curve of the sample annealed at 600 K is very similar to that of the as-prepared sample (Fig. 5b). A remarkable shift of the scattering curve indicating the increase in the volume fraction of the second

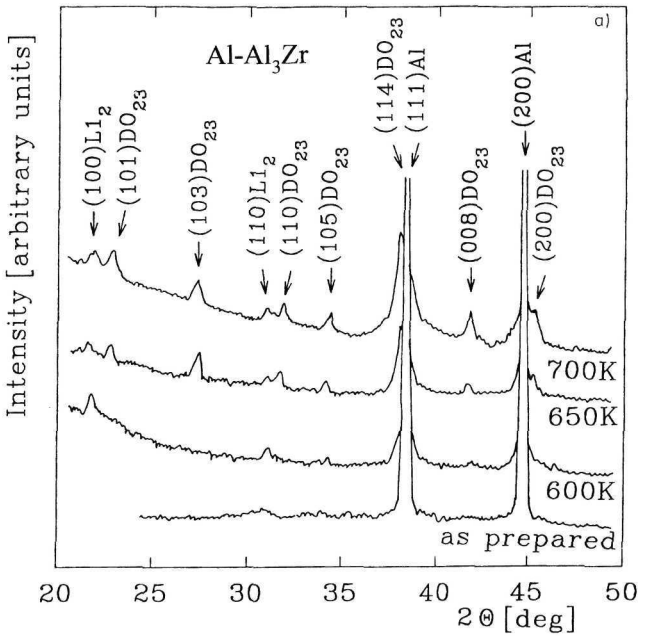
a)
Al-Al3Zr
(100)L12
(101)DO23
(103)DO23
(110)L12
(110)DO23
(105)DO23
(114)DO23
(111)Al
(008)DO23
(200)Al
(200)DO23
700K
650K
600K
as prepared
Intensity [arbitrary units]
20
25
30
35
40
45
50
2Θ [deg]

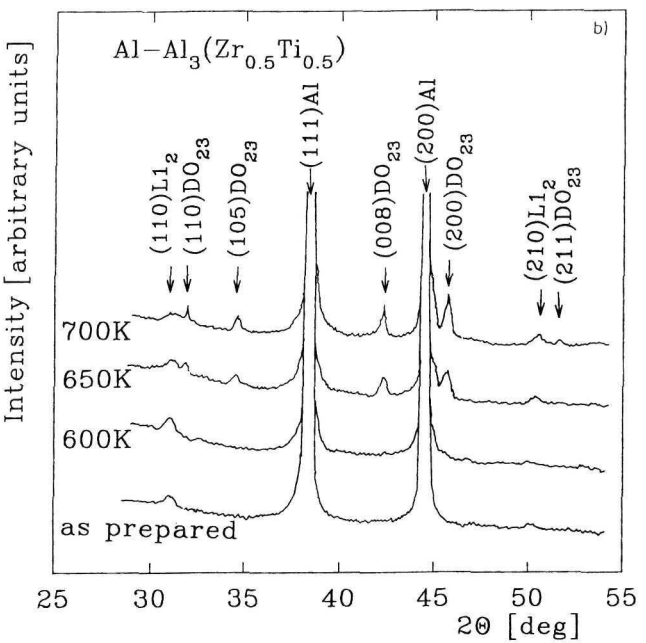
b)
Al−Al3(Zr0.5Ti0.5)
(110)L12
(110)DO23
(105)DO23
(111)Al
(008)DO23
(200)Al
(200)DO23
(210)L12
(211)DO23
700K
650K
600K
as prepared
Intensity [arbitrary units]
25
30
35
40
45
50
55
2Θ [deg]

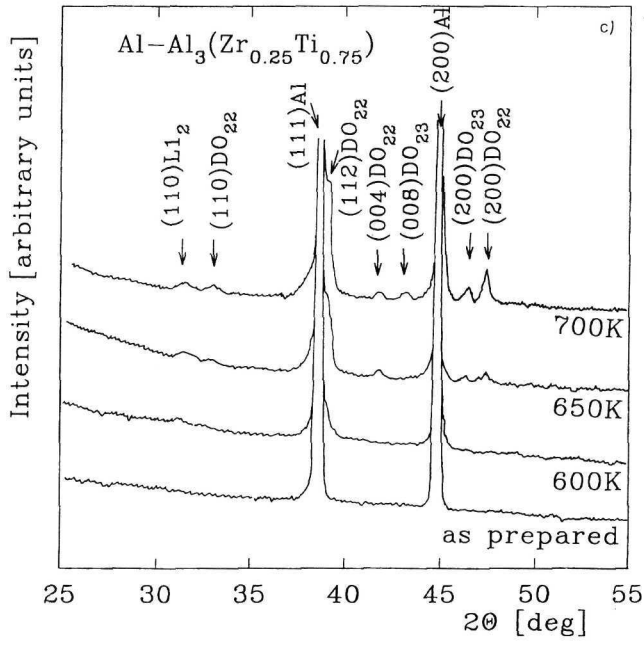

Fig. 6. X-ray diffractograms of selected Al-$Al_3(Zr_xTi_{1-x})$ alloys annealed at different temperatures: a) $x = 1$, $t = 100$ h, b) $x = 0.5$, $t = 500$ h, c) $x = 0.25$, $t = 500$ h.

phase particles is shifted to the annealing temperature of 650 K. A gradual slight shift of SAXS curves was found in the Al-Al_3Ti alloy (Fig. 5c).

The changes in the phase composition of the Al-Zr-Ti alloys during their long term annealing at elevated temperatures were studied by means of the X-ray diffraction method. As the structures of the non-matrix phases which are expected to be formed during this annealing are very similar to that of the matrix, the most intensive diffraction peaks of these phases are overlapped by the matrix peaks. Only some less intensive diffraction extra peaks resulting from the ordering of these phases might be observed. Fig. 6a shows the diffractograms of the binary Al-Zr alloy annealed at different temperatures for 100 hours. While the as-prepared sample exhibits, in addition to the matrix peaks, only one small and very diffuse peak at the position corresponding to the (110) reflection of the metastable Al_3Zr phase, annealing at 600 K results in an intensity increase of reflections of the metastable Al_3Zr phase and slight undulations are found at positions corresponding to the reflections of the stable Al_3Zr phase. These undulations are replaced by ordinary peaks if the annealing temperature is increased to 650 K. Further increase in the an-

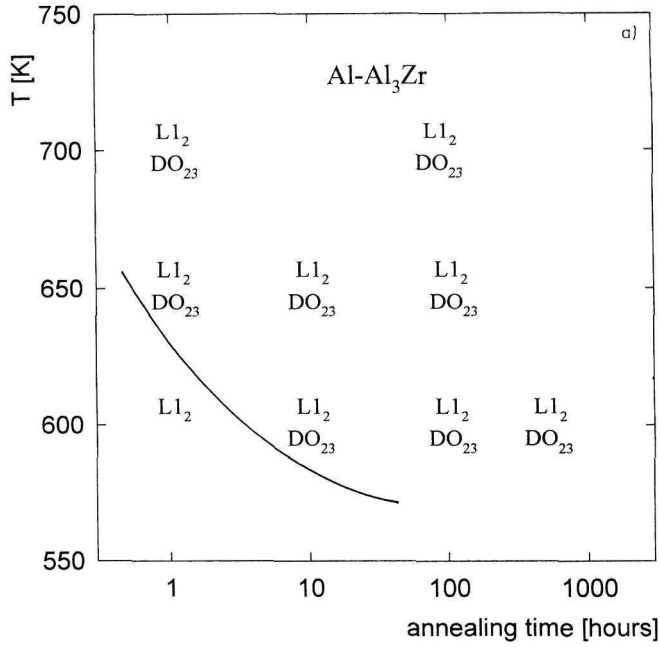
a)
Al-Al3Zr
T [K]
750
700
650
600
550
L12
DO23
1
10
100
1000
annealing time [hours]

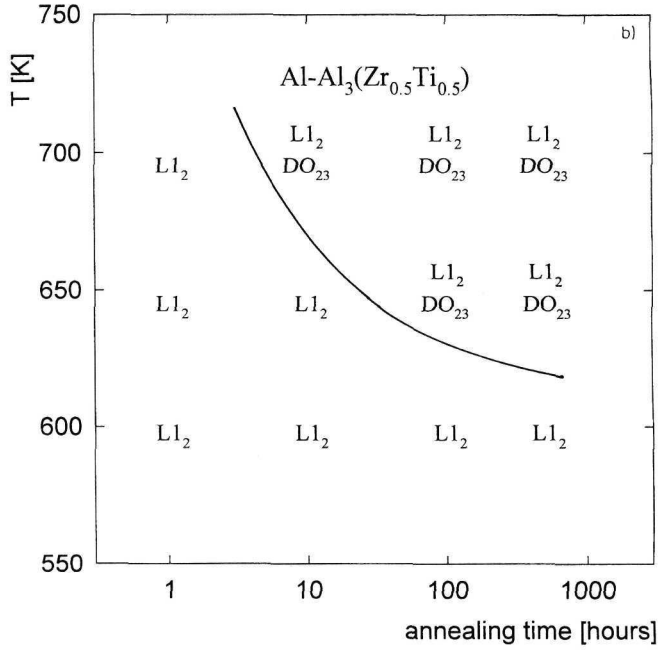
b)
Al-Al3(Zr0.5Ti0.5)
T [K]
750
700
650
600
550
L12
DO23
1
10
100
1000
annealing time [hours]

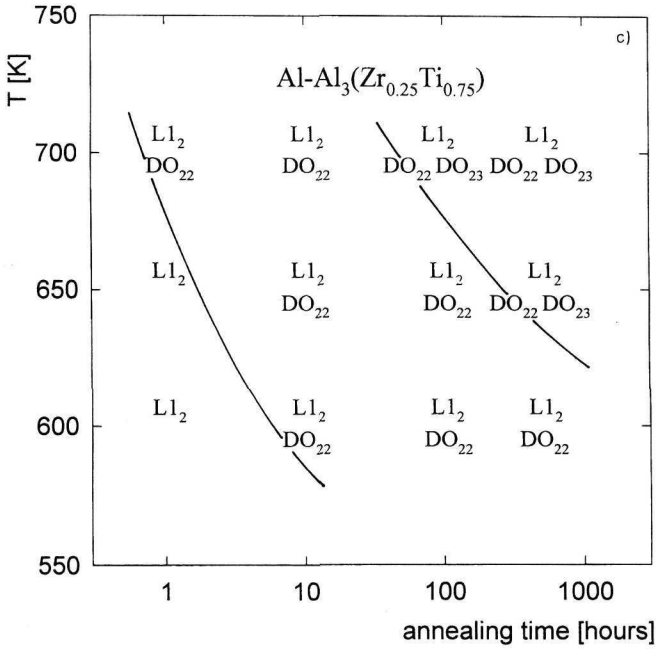

Fig. 7. Transformation diagrams for selected Al-$Al_3(Zr_xTi_{1-x})$ alloys: a) $x = 1$, b) $x = 0.5$, c) $x = 0.25$.

nealing temperature enhances the intensity of reflections of the stable Al_3Zr phase, however, the reflections of the metastable Al_3Zr phase are still present. Fig. 6b shows the diffractograms of the Al-$Al_3(Zr_{0.5}Ti_{0.5})$ alloy annealed at different temperatures for 500 hours. The sequence of the decomposition of the supersaturated matrix is similar to that found in the binary Al-Zr alloy. The formation of the stable DO_{23} phase was, however, observed only after annealing at temperatures $T \geq 650$ K. A much lower tendency to the formation of the metastable $L1_2$ phase was found in the Al-$Al_3(Zr_{0.25}Ti_{0.75})$ annealed for 500 hours at different temperatures (Fig. 6c). The formation of the stable DO_{23} phase is preceded by the formation of the stable DO_{22} phase. All above mentioned phases were observed in the sample annealed at 700 K.

The results of the X-ray diffraction analysis were used for the construction of the transformation diagrams showing the presence of individual phases after different combinations of annealing temperatures and annealing times. Fig. 7 shows that the boundary between the region where only the metastable $L1_2$ phase is detected and the region where the metastable $L1_2$ and stable DO_{23} phases co-exist

simultaneously moves to higher temperatures or longer times with increasing Ti content.

A careful inspection of the positions of diffraction peaks shows that the lattice parameters of both metastable $L1_2$ and stable DO_{23} modifications of the $Al_3(Zr_xTi_{1-x})$ phase depend on the stoichiometric parameter x (compare e.g. the (200) DO_{23} peaks in Figs. 6a and 6b). The lattice parameters of both phases which do not depend on the annealing conditions are given in Table 3 and compared with the interpolated values obtained from the data [12].

Table 3. Measured lattice parameters a_{exp} and c_{exp} of the $Al_3(Zr_xTi_{1-x})$ phases and their comparison with parameters a_{th} and c_{th} interpolated from literature data

x	$L1_2$		DO_{23}			
	a_{exp} [nm]	a_{th} [nm]	a_{exp} [nm]	a_{th} [nm]	c_{exp} [nm]	c_{th} [nm]
0.75	0.405 ± 0.001	0.4050	0.398 ± 0.001	0.398	1.717 ± 0.003	1.720
0.5	0.404 ± 0.001	0.4022	0.396 ± 0.001	0.395	1.707 ± 0.003	1.707
0.25	0.399 ± 0.001	0.3994	0.392 ± 0.001	0.392	1.682 ± 0.003	1.695

4. Discussion

The electrical resistance R is a product of the resistivity ζ and the formfactor F

$$R = F\zeta, \tag{4}$$

where both ζ and F depend on temperature. However, the temperature dependence of F is much weaker and the measured temperature dependence of R characterises well the temperature dependence of ζ. The resistivity of metallic materials may be expressed as

$$\zeta(T) = \zeta_{lat}(T) + \zeta_{def}(T), \tag{5}$$

where $\zeta_{lat}(T)$ is the resistivity of an ideally pure metal without any lattice defects (in the first approximation it depends linearly on temperature) and $\zeta_{def}(T)$ represents the contribution of lattice defects (point defects, dislocations, grain boundaries, second phase particles). If the scattering centres corresponding to individual lattice defects do not interact and their concentrations are low, the term $\zeta_{def}(T)$ may be expressed as

$$\zeta_{def}(T) = \sum_i c_i(T)\Delta\zeta_i, \tag{6}$$

where $c_i(T)$ are the concentrations of individual lattice defects at the temperature T and $\Delta\zeta_i$ are considered to be temperature independent constants. Any structure

changes occurring during annealing result in the changes of corresponding defects concentrations c_i and in the deviation of the $\zeta(T)$ dependence from linearity.

The structure of the as-melt-spun Al-Zr-Ti alloys is fine grained with a very low dislocation density [7, 16] and does not change significantly during the heat treatment used in our experiments. The estimated contributions of dislocations and grain boundaries to resistivity may be neglected. The main contribution to the resistivity of as-melt-spun Al-Zr-Ti alloys may be expected from Zr and Ti atoms which are dissolved in the supersaturated matrix [7]. The contribution of second phase particles to resistivity is generally significantly lower than that of solute atoms. Precipitation should thus lead to a decrease in resistivity whereas the dissolution of particles to its increase.

The irreversible resistance drop which occurs predominantly during the first heating may be explained by the decomposition of the supersaturated Al-based matrix. A precise analysis of the resistance data is difficult because of the uncertainty in the formfactor F (due to variable width and thickness of the sample). A rough estimate of the sample dimensions in the binary Al-Zr alloy gives $F = 6 \times 10^5$ m and the resistivities measured at 300 K are $\zeta = 7.7 \times 10^{-8}$ Ω m in the as-melt-spun state and $\zeta = 3.3 \times 10^{-8}$ Ω m after the second heat treatment cycle. The latter value is slightly higher than that for pure Al (between 2.4 and 2.7×10^{-8} Ω m). This difference may be explained by the contribution of the second phase particles. The repeated experiments showed that the Al-Zr sample was close to the thermodynamic equilibrium after two heat treatment cycles, i.e. a negligible amount of Zr is dissolved in the matrix. The resistivity measured in our Al-Zr sample is also close to the value of 3.15×10^{-8} Ω m reported in [2] for the equilibrium Al-1wt.%Zr alloy. Much higher resistivity found in the as-melt-spun state reflects predominantly the contribution of dissolved Zr atoms. According to the SAXS and X-ray diffraction experiments [7] the as-melt-spun Al-Zr alloy should contain about 1.5 vol.% of the Al_3Zr phase and the remaining Zr atoms (about 2.9 wt.%) should be dissolved in the matrix. The resistivity drop $\Delta\zeta = 4.4 \times 10^{-8}$ Ω m occurring during two heat treatment cycles should thus correspond to the release of this amount of Zr from the solution. The diversity of existing literature data on the influence of the Zr atoms on resistivity of Al [2] exclude any reasonable quantitative comparison with our results.

The two stage character of the irreversible resistivity drop observed during the first heating of the Al-Zr alloy (Fig. 4) suggests the operation of two processes – the first operating with a maximum rate at temperature about 630 K and the second one operating at temperatures of about 50 K higher. Numerous experiments performed with binary Al-Zr alloys show that the formation of the stable Al_3Zr phase (structure type DO_{23}) is preceded by the formation of the metastable modification of the same stoichiometry (structure type $L1_2$) (e.g. [3, 4]). The X-ray diffraction analysis confirmed such a decomposition sequence to occur also in our Al-Zr alloy.

The metastable $L1_2$ phase is present already in the as-melt-spun ribbons. However, an increase in the intensity of its diffraction peaks after annealing at 600 K suggests an increase in its volume fraction. This annealing temperature coincides well with the temperature at which the first stage of decomposition was found by resistance measurements. The formation of the metastable $L1_2$ modification of the Al_3Zr phase is considered to be responsible for the first stage of decomposition. The transformation diagram constructed on the base of X-ray diffraction analysis (Fig. 7) reveals that at short annealing times the stable DO_{23} modification of the Al_3Zr phase may be detected at temperatures close to about 650 K. This temperature coincides well with the temperature where the second stage of decomposition was found in the resistivity measurements. The formation of the stable DO_{23} modification of the Al_3Zr phase is, therefore, believed to be responsible for the resistivity changes in the second stage of decomposition.

The second important feature of the $R(T)$ curve measured in the Al-Zr alloy is its reversible deviation from linearity at high temperatures (above about 600 K). The redissolution of the second phase particles controlled by the temperature dependence of the equilibrium solid solubility of Zr in Al is believed to be the reason for this effect. The value of this deviation was determined at 800 K and reaches about 10% of the total resistivity drop observed during two heat treatment cycles. Assuming that the total drop in resistivity corresponds to the redistribution of about 3 wt.% of Zr atoms and that the dependence of resistivity on the solute content is usually weaker than linear, the resistivity change observed at 800 K should correspond to the redistribution of less than about 0.2 wt.% of solute atoms. This estimate agrees well with the expected change in the solubility limit of Zr in Al with temperature.

A partial substitution of Ti for Zr in the Al-Zr-Ti alloys does not change the general character of $R(T)$ curves but modifies both the position and the extent of particular decomposition stages (Figs. 3, 4). A precise quantitative comparison of the decomposition behaviour of these alloys is not possible because the formfactors of individual alloys are not available. In order to make at least a rough estimate, we supposed that the volume fractions of the second phase particles after two heat treatment cycles were the same in all Zr-containing Al-Zr-Ti alloys and, therefore, also the resistivity values after two heat treatment cycles were supposed to be the same as in the binary Al-Zr alloy. Under this assumption the formfactors of individual Al-Zr-Ti alloys were estimated and the resistance values measured were converted into resistivity values.

The resistivity drop observed during two heat treatment cycles decreases with decreasing Zr content ($\Delta\zeta = 4.4 \times 10^{-8}$ Ω m for $x = 1$, $\Delta\zeta = 2.5 \times 10^{-8}$ Ω m for $x = 0.5$, $\Delta\zeta = 1.7 \times 10^{-8}$ Ω m for $x = 0.25$). Three points may be considered to explain this effect:

– the volume fraction of the second phase particles which are present already

in the as-melt-spun alloys increases with decreasing Zr content, i.e. a lower amount of solute atoms is redistributed during the decomposition (this explanation seems to be supported by the results of SAXS experiments [7]);

– the influence of dissolved Ti atoms on the resistivity of Al is weaker than that of Zr atoms (no reliable literature data are available for the comparison);

– the decomposition rate decreases with decreasing Zr content. The decomposition of alloys with a lower Zr content and higher Ti content (lower x) is, therefore, only partial and the measured value of $\Delta\zeta$ does not correspond to the complete decomposition.

The third hypothesis may be supported by the comparison of the resistivity drops $\Delta\zeta^{\mathrm{I}}$ and $\Delta\zeta^{\mathrm{II}}$ observed during the first and the second heat treatment cycles, respectively. While about 98% of the total resistivity drop occurs during the first cycle in the Al-Zr alloy, this contribution decreases to about 92% in the alloy with $x = 0.25$. The idea of a decreasing decomposition rate is also supported by the shift of particular decomposition stages to higher temperatures with decreasing Zr content and increasing Ti content (Fig. 4). Similar conclusions may be drawn from the SAXS experiments which also show a delay in the increase of volume fraction of the second phase particles due to the substitution of Ti for Zr.

The explanation of the decomposition stages suggested for the Al-Zr alloy seems to be valid also for other Zr-rich ($x \geq 0.5$) Al-Zr-Ti alloys. The position of the first stage of decomposition corresponds well with the temperature range where the intensity of the diffraction peaks of the $L1_2$ modification of the $Al_3(Zr_xTi_{1-x})$ phase increases. Similarly, the shift of the second decomposition stage to higher temperatures with decreasing parameter x corresponds well with the shift in the appearance of diffraction peaks of the DO_{23} modification of the $Al_3(Zr_xTi_{1-x})$ phase (Fig. 7). The good correspondence between the measured lattice parameters of both modifications of the $Al_3(Zr_xTi_{1-x})$ phase and the interpolated values computed from the lattice parameters of both binary Al_3Zr and Al_3Ti phases confirms that the Ti atoms really substitute the Zr atoms in the lattice of the $Al_3(Zr_xTi_{1-x})$ phases and the content of Zr and Ti atoms in these phases agrees well with the desired values.

The decomposition behaviour of the Ti-rich Al-Zr-Ti alloys ($x \leq 0.25$) is somewhat different. The $R(T)$ curves exhibit much smaller irreversible drops of resistance and are shifted to higher temperatures. The decomposition rate is significantly slower than that in the Zr-rich alloys. The intensity of diffraction peaks of the $L1_2$ modification of the $Al_3(Zr_xTi_{1-x})$ phase is much smaller and the particles of the stable modification of the $Al_3(Zr_xTi_{1-x})$ phase have predominantly the DO_{22} structure in the alloy with $x = 0.25$, i.e. the structure typical of the Al_3Ti system. The formation of the DO_{23} phase is very limited and shifted to much higher temperatures as compared with the Zr-rich alloys. The coexistence of both phases agrees with data obtained in alloys of similar composition [17, 18].

The metastable $L1_2$ $Al_3(Zr_xTi_{1-x})$ phase is believed to be the main strengthening phase in the Al-Zr-Ti alloys developed for elevated temperature applications. A partial substitution of Zr atoms by Ti ones enables to reduce the lattice mismatch between the $Al_3(Zr_xTi_{1-x})$ particles and the matrix to zero (for $x \cong 0.7$). This should reduce the rate of particle coarsening and, thus, also the rate of softening during a long term exposure to elevated temperatures. However, the coarsening of the $L1_2$ $Al_3(Zr_xTi_{1-x})$ particles is not the sole process which may contribute to a softening at elevated temperatures. The formation of the stable modification of the $Al_3(Zr_xTi_{1-x})$ phase may be even more important as both the size and the lattice mismatch of its particles are significantly higher in comparison with the $L1_2$ phase. The shift of the stable phase formation to higher temperatures with increasing Ti content may be even more important than the influence of Ti on the lattice mismatch of the $L1_2$ phase. The investigation of the strengthening phases morphology and the measurement of microhardness is necessary to verify this idea. The results of this investigation will be presented in the next paper.

5. Conclusions

1. An irreversible drop of resistivity occurs during the first annealing of the Al-Zr-Ti alloys and may be explained by the decomposition of the supersaturated matrix. The first stage of this decomposition may be interpreted as the formation of the metastable $Al_3(Zr_xTi_{1-x})$ phase with cubic $L1_2$ structure. The second stage probably relates to the formation of the stable $Al_3(Zr_xTi_{1-x})$ phase with tetragonal DO_{23} (for $x \geq 0.5$) or DO_{22} (for $x \leq 0.25$) structures.

2. The Ti atoms substitute for Zr atoms in the lattice of both stable and metastable $Al_3(Zr_xTi_{1-x})$ phases and the chemical compositions of both phases agree well with nominal compositions. The presence of Ti atoms in the lattice of the $Al_3(Zr_xTi_{1-x})$ phases modifies their lattice mismatch to the Al-based matrix and a zero mismatch of the $L1_2$ phase may be achieved for the stoichiometric parameter $x \cong 0.7$.

3. The decomposition of the supersaturated matrix is shifted to higher temperatures by addition of Ti. Especially the shift of the second stage, i.e. the delay in the formation of the stable $Al_3(Zr_xTi_{1-x})$ phase, is expected to be of extraordinary importance for the retaining of a high strength during the exposure of Al-Zr-Ti alloys to elevated temperatures.

Acknowledgements

The authors are grateful to Dr. D. Plischke, Crystal Laboratory Göttingen, Germany, for the preparation of thin ribbons and to Ing. L. Dobiášová for the help with X-ray measurements. The research was supported by the Grant Agency of the Charles University through the grant No. 283 and by the Grant Agency of the Czech Republic through the grant No. 93-2432.

REFERENCES

[1] WATTS, B. M.—STOWELL, M. J.—BAIKIE, B. L.—OWEN, D. G. E.: Metal. Sci. J., *10*, 1976, p. 189.
[2] MONDOLFO, L.: In: Aluminium Alloys: Structure and Properties. London, Butterworth 1976.
[3] PANDEY, S. K.—GANGOPADHYAY, D. K.—SURYANARAYANA, C.: Z. Metallkde, *77*, 1986, p. 12.
[4] CHAUDHURY, Z. A.—SURYANARAYANA, C.: Metallography, *17*, 1984, p. 231.
[5] CHU, M. G.: Mater. Sci. Eng. A, *179/180*, 1994, p. 669.
[6] NIE, J. E.—MAJUMDAR, A.—MUDDLE, B. C.: Mater. Sci. Eng. A, *179/180*, 1994, p. 619.
[7] MÁLEK, P.—BARTUŠKA, P.—PLEŠTIL, J.: Kovove Mater., *37*, 1999, p. 386.
[8] LIFSHITZ, I. M.—SLYOZOV, V. V.: J. Phys. Chem. Solids, *19*, 1961, p. 35.
[9] WAGNER, C.: Z. Elektrochem., *65*, 1961, p. 581.
[10] BRAUER, G.: Z. Anorg. Allgem. Chem., *242*, 1939, p. 1.
[11] NES, E.: Acta Metall., *20*, 1972, p. 499.
[12] SRINIVASAN, S.—DESCH, P. B.—SCHWARZ, R. B.: Scripta Metall. Mater., *25*, 1991, p. 2513.
[13] ZEDALIS, M.—FINE, M. E.: Met. Trans. A, *17*, 1986, p. 2187.
[14] SPRUŠIL, B.—ŠÍMA, V.—CHALUPA, B.—SMOLA, B.: Z. Metallkd., *118*, 1993, p. 84.
[15] KRATKY, O.: Prog. Biophys., *13*, 1963, p. 105.
[16] MÁLEK, P.—JANEČEK, M.—SMOLA, B.—BARTUŠKA, P.: Kovove Mater., *38*, 2000, p. 9.
[17] TSUNEKAWA, S.—FINE, M. E.: Scripta Metall., *16*, 1982, p. 391.
[18] PARK, S. I.—HAN, S. Z.—CHOI, S. K.—LEE, H. M.: Scripta Mater., *34*, 1996, p. 1697.

Received: 19.4.1999